AD-A132 403 MATHEMATICAL MODELS OF NONLINEAR GALVANIC POLARIZATION (U) NAVAL UNDERWATER SYSTEMS CENTER NEW LONDON CT NEW LONDON LAB R G KASPER ET AL. 16 AUG 83 NUSC-TR-6921 1/1

UNCLASSIFIED F/G 12/1 NL

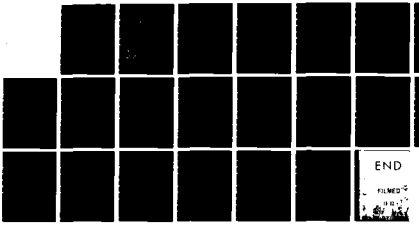

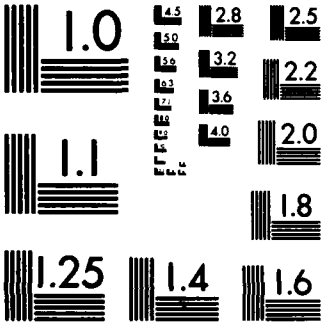

NUSC Technical Report 6921
16 August 1983

Mathematical Models of Nonlinear Galvanic Polarization

Rolf G. Kasper
Michael O. Duffy
Engineering and Technical Support Department

Naval Underwater Systems Center
Newport, Rhode Island / New London, Connecticut

Preface

This work was sponsored by the Office of Naval Research, Program Element 61153N, NR Number 036-163-(675-021X) and Research Projects RR014-11-0B and RR022-08-01. The Program Manager for this research is Dr. P. Clarkin, Code 431. This research project is entitled *Pitting and Crevice Corrosion Kinetics.* The Principal Investigator is Dr. R. G. Kasper, Code 4493.

The authors gratefully acknowledge the helpful discussions with R. S. Munn.

The Technical Reviewer for this report was R. S. Munn, Code 44.

Reviewed and Approved: 16 August 1983

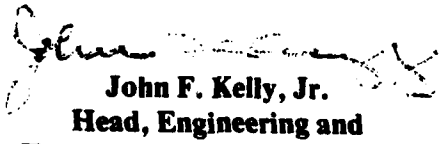

John F. Kelly, Jr.
Head, Engineering and
Technical Support Department

The authors of this report are located at the
New London Laboratory, Naval Underwater Systems Center,
New London, Connecticut 06320.

REPORT DOCUMENTATION PAGE

READ INSTRUCTIONS BEFORE COMPLETING FORM

1. REPORT NUMBER: TR 6921	2. GOVT ACCESSION NO.: AD-A132403
3. RECIPIENT'S CATALOG NUMBER:	
4. TITLE (and Subtitle): MATHEMATICAL MODELS OF NONLINEAR GALVANIC POLARIZATION	5. TYPE OF REPORT & PERIOD COVERED: Interim Report
	6. PERFORMING ORG. REPORT NUMBER: TR 6921
7. AUTHOR(s): Rolf G. Kasper Michael O. Duffy	8. CONTRACT OR GRANT NUMBER(s): NR 036-163(675-021X)
9. PERFORMING ORGANIZATION NAME AND ADDRESS: Naval Underwater Systems Center New London Laboratory New London, Connecticut 06320	10. PROGRAM ELEMENT, PROJECT, TASK AREA & WORK UNIT NUMBERS: 61153N
11. CONTROLLING OFFICE NAME AND ADDRESS: Chief of Naval Research Office of Naval Research Arlington, VA 22217	12. REPORT DATE: 16 August 1983 13. NUMBER OF PAGES: 28
14. MONITORING AGENCY NAME & ADDRESS (if different from Controlling Office): Chief of Naval Research Office of Naval Research Arlington, VA 22217	15. SECURITY CLASS. (of this report): UNCLASSIFIED 15a. DECLASSIFICATION / DOWNGRADING SCHEDULE:

16. DISTRIBUTION STATEMENT (of this Report)
Approved for public release; distribution unlimited.

17. DISTRIBUTION STATEMENT (of the abstract entered in Block 20, if different from Report)

18. SUPPLEMENTARY NOTES

19. KEY WORDS (Continue on reverse side if necessary and identify by block number)

Analytical/empirical correlation	Nearfield electrode measurements
Corrosion pitting	Nonlinear anodic polarization
Current density predictions	Nonlinear cathodic polarization
Electric potential distribution	

20. ABSTRACT (Continue on reverse side if necessary and identify by block number)

The basic differential equation governing the conductive-current flow in an electrical continuum is analogous to the general heat-conduction equation. A series of simple steady-state electrochemical models were created using the COSMIC/NASTRAN finite-element program. The purpose of this study is to observe the behavior, physically and mathematically, of convective membrane boundary elements when assigned a nonlinear current-flow capability with respect to the local surface electric potential. Nodal potentials and current flows for a

DD FORM 1 JAN 73 1473

20. (Cont'd)

variety of boundary conditions and model configurations are given and modeling conclusions based on this analysis are presented.

TABLE OF CONTENTS

LIST OF ILLUSTRATIONS

LIST OF TABLES

MATHEMATICAL MODELS OF NONLINEAR GALVANIC POLARIZATION

INTRODUCTION

Serious corrosion problems have affected the hardware of the commercial and military communities for many years. It has been estimated that a significant percentage of the U.S. gross national product is lost annually because of ineffective cathodic protection. Corrosion problems in the commercial sector are found in the automotive and oil industries; corrosion problems in the military sector are found in the inadequate protection of hulls, propellers, engines, torpedoes, missiles, etc.

This study will develop a numerical model that describes the gradual corrosion of a surface from a planar to a pitted contour. The model will provide corrosion information such as that found in figure 1, where pitting is shown as a function of time and geometry. The model relies for its predictions on established scientific laws (conservation of charge and Faraday's) and a fixed set of physical parameters. The parameters are chosen to provide information on potential and current distributions within the electrolyte and on the anodic and cathodic surfaces. Sufficient measurements are taken under controlled conditions to ensure that the chosen electrochemical parameters

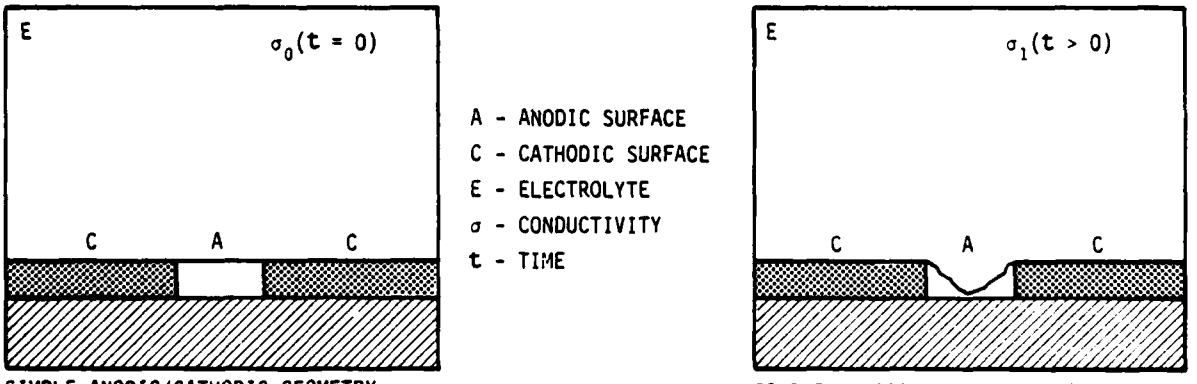

SIMPLE ANODIC/CATHODIC GEOMETRY
ELECTROLYTIC CONDUCTIVITY CONSTANT

COMPLEX ANODIC/CATHODIC GEOMETRY
UPDATED ELECTROLYTIC CONDUCTIVITY

Figure 1a. Virgin State at t = 0 Figure 1b. Evolved State at t > 0

Figure 1. Corrosion Pitting as a Function of Time and Geometry

result in predictions that compare to reality. Periodic potentiostatic polarization and impedance measurements are required to update model parameters to reflect accurately the state of the pitting process.

This work integrates the geometric and electrolytic evolution with time into numerical models (finite-element method) capable of predicting localized corrosion kinetics. The numerical models use empirical information to initiate the predictive process. This report focuses on the mathematical treatment of a general nonlinear polarization layer consistent with the appropriate conservation laws.

BACKGROUND

The characterization of localized corrosion phenomena, such as pitting and crevice corrosion, has been studied for years.[1-3] Mathematical prediction of electrolytic corrosion behavior for a physical situation had its genesis at least four decades ago. Traditional mathematical techniques were reviewed for predicting the potential fields of anodes and cathodes in the presence of geometric effects, polarization curves, surface roughness, etc.[4] Analytical attempts to calculate local current distributions in the anodic/cathodic neighborhood (surfaces) demonstrated the intractability of exact mathematical solutions.[5]

In recent years, attempts have been made to model localized corrosion through use of detailed models of the electrochemistry in localized regions. These models were limited to simple geometries and constant electrolytic properties.[6-9] The models were further limited because the analyses did not consider either geometric changes or changes in composition and conductivity of the electrolyte during corrosion.

Recent studies have applied the finite-element numerical technique to macroscopic electrogalvanic field predictions. These models were developed to predict performance of cathodically protected structures.[10-15] Again, the models did not consider changes in geometry and electrolytic properties. However, they were successful in predicting macroscopic current distributions at the various anodic and cathodic areas.

This study investigates the use of nonlinear analysis within a subsystem of the NASA Structural Analysis (COSMIC/NASTRAN) program (Heat Transfer, Rigid Format 3) to address complex electrode boundary conditions and electrolytic interactions for the beaker model. A parallel effort, studying the potential strength of a more general nonlinear finite-element program known as MARC, is also in progress.[16] Both finite-element programs are maintained on a VAX-11/780 computer at the Naval Underwater Systems Center (NUSC).

A number of papers demonstrate that localized changes in the electrolyte chemistry occur with time and geometry during corrosion.[6] It is, therefore, important to include these phenomena in any model dealing with localized corrosion kinetics.

APPROACH

The approach to this research effort is two phased. First, numerical models are developed to describe the gradual corrosion of a surface from a planar to a pitted contour. The model provides corrosion information such as that found in figure 1, where pitting is shown as a function of time and geometry. The model relies for its predictions on established scientific laws (conservation of charge and Faraday's) and a fixed set of physical parameters. The parameters are chosen to provide information on potential and current distributions within the electrolyte and on the anodic and cathodic surfaces.

In conjunction with this effort, sufficient measurements are taken to ensure the chosen electrochemical parameters result in predictions that will compare with reality. These measurements are made under controlled laboratory conditions by Dr. C. R. Crowe, of the Naval Surface Weapons Center (NSWC). Periodic potentiostatic polarization and impedance measurements are also required to update model parameters to reflect accurately the state of the pitting process.

This report emphasizes the evaluation of existing finite elements for nonlinear applications. A number of finite elements residing within COSMIC/NASTRAN computer code are tested for mesh sizing, accuracy of nonlinear (table input) membrane response, and various anodic and cathodic boundary conditions.

PHYSICAL CONSIDERATIONS

The introduction of mixed-potential theory appeared in literature some 40 years ago.[17] The theory states that any electrochemical reaction can be divided into two or more oxidation and reduction reactions. It negates the existence of net-charge accumulation during an electrochemical reaction. The significance of these statements is that electrically coupled metals in an electrolyte behave in a totally different manner than the same metals in electrical isolation.

The oxidation-reduction curves for each metal are determined in the laboratory for the steady-state potential of the metal in an electrolyte. Figure 2 demonstrates this case for zinc, copper, and iron in salt water (3 percent NaCl) at 30°C when measured in reference to a standard electrode, usually a saturated calomel electrode (SCE) or a silver/silver-chloride (Ag/AgCl) electrode. These polarization curves measure the nonlinear transition between two potential states and associated current density states. These curves characterize the various electrochemical reactions for an electrode independent of exterior global, or large-scale, conditions. This fundamental assumption allows the analyst to apply measured laboratory uncoupled electrochemical information to define the electrical sources and sinks for a given boundary-value problem.

A fundamental assumption in this finite-element analysis is that the base-metal substrate has a uniform electrical potential.[12] The basis of this

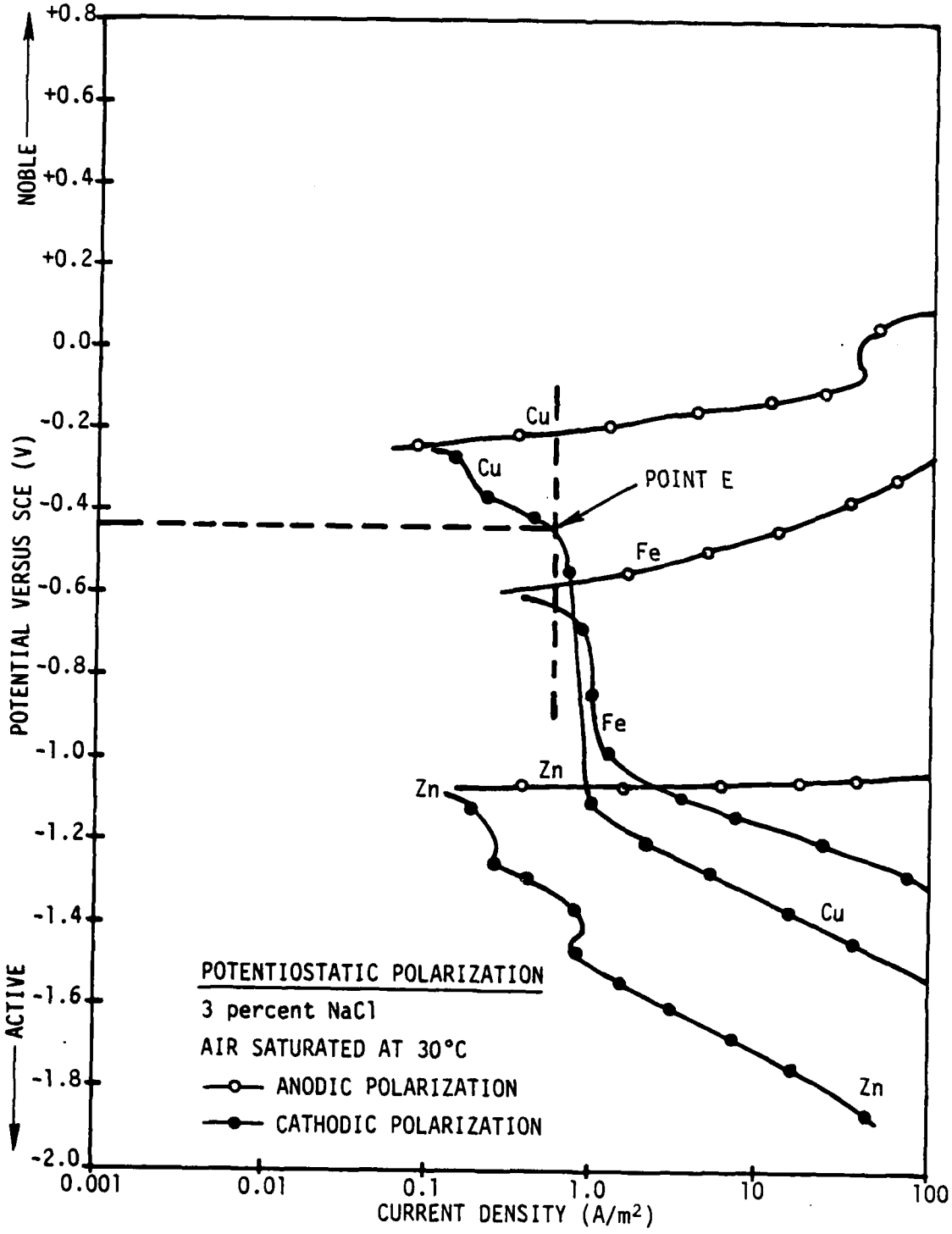

Figure 2. Polarization Curves

assumption is that a base-metal substrate has high conductivity compared to that of the electrolyte and can, therefore, support large current values for small potential differences.

Although the metal substrate potential is assumed to be uniform, a potential difference between the base-metal substrate and the electrolyte of the metal may vary considerably. (This difference is due to paint or polarization layers and can be measured by a reference cell.) The potential difference measured at a zinc surface, for instance, is certainly different from that measured at exposed iron or copper areas.

THEORETICAL CONSIDERATIONS

A general finite-element modeling (FEM) procedure for calculating ele .o- galvanic field responses due to multiple anodic/cathodic interactions has n developed for macroscopic galvanic current-density assessment.[14-15] The a ic/cathodic interactions in the conductive electrolyte are predicted by th application of classical dc electric-field theory for conductive continuums in conjunction with widely accepted laboratory oxidation/reduction responses for the electrodes. The electrogalvanic fields in the electrolyte are calculated with the scalar Poisson equation, whereby traditional boundary conditions are prescribed in the farfield of the electrolyte. In the nearfield of the anodes, cathodes, and the painted metallic substrate, complex boundary conditions are enforced based on empirical polarization curves and paint-impedance values. The ionic current in the electrolyte, leaving the anode and arriving at the cathodes, is mathematically constrained to sum to zero over the metallic surface (spatial Kirchhoff's law).

Generally, electric-current flow in a conducting medium is governed by the law of conservation of charge. In differential equation form, this law can be stated as

$$\nabla \cdot \bar{J} = - \frac{\partial \rho}{\partial t} . \tag{1}$$

The constitutive relationship (Ohm's law) between current density and the electric-field intensity, in terms of electrical conductance, is

$$\bar{J} = \sigma \bar{E} , \tag{2}$$

where, by definition, the electric-field intensity is

$$\bar{E} = -\nabla \phi . \tag{3}$$

Substitution of equations (3) and (2) into equation (1) yields

$$\nabla \cdot \sigma \nabla \phi = - \frac{\partial \rho}{\partial t} . \tag{4}$$

This basic differential expression governing the conductive-current flow in an electrical continuum is analogous to the general heat-conduction equation. Specifically, the heat-conduction equation can be stated as

$$\nabla \cdot k\nabla T + \dot{q} = \rho_m C_h (\partial T/\partial t) \quad . \tag{5}$$

Table 1 illustrates the specific analogous independent and dependent variables relating equations (4) and (5). The above analogy provides the analyst with a mathematical tool (FEM) that exists on numerous finite-element computer codes. Many linear applications have already been demonstrated using equation (5).

A need exists to incorporate mathematically the complex nonlinear polarizations at the various electrode-electrolyte interfaces into the field equation, equation (1); the constitutive equation, equation (2); and the conservation equation, equation (4).

MODEL EVOLUTION AND DEVELOPMENT

Various FEM's were generated to check out (1) different elements, (2) nonlinear responsiveness by means of table input routines, and (3) boundary conditions (single-point constraint (SPC), multipoint constraint (MPC), enforced potentials, and enforced currents).

Figure 3 shows the FEM of a steady-state and two-dimensional electrostatic problem. The model consists of two four-noded quadrilateral elements with one degree of freedom per node. The electrical conductivity of each element is assumed to be constant. The horizontal sides of the model are assumed to be insulated. The left nodes are held at a constant electrical potential. The right nodes are connected to another fixed-potential state by one of the boundary elements under investigation, thereby creating a potential difference.

Three different COSMIC/NASTRAN elements were used to model the solid-fluid interface: (1) CELAS2, (2) CQDMEM, and (3) CHBDY. The CELAS elements, spring elements, performed satisfactorily. However, the element is better suited for structural than electrical applications. The electrical conductivity must be

Table 1. Comparison of Variables

Thermal Variable	Nomenclature	Electrogalvanic Variable
K	Thermal, electrical conductivity	σ
T	Temperature, electric potential	ϕ
$-\nabla T$	Negative gradient	$-\nabla\phi = \bar{E}$
$-K\nabla T$	Flux, current density	$-\sigma\nabla\phi = \bar{J}$
$-\dot{q}$	Negative time-dependent source	$(\partial\rho/\partial t)$
Q	Total heat, current flow	I

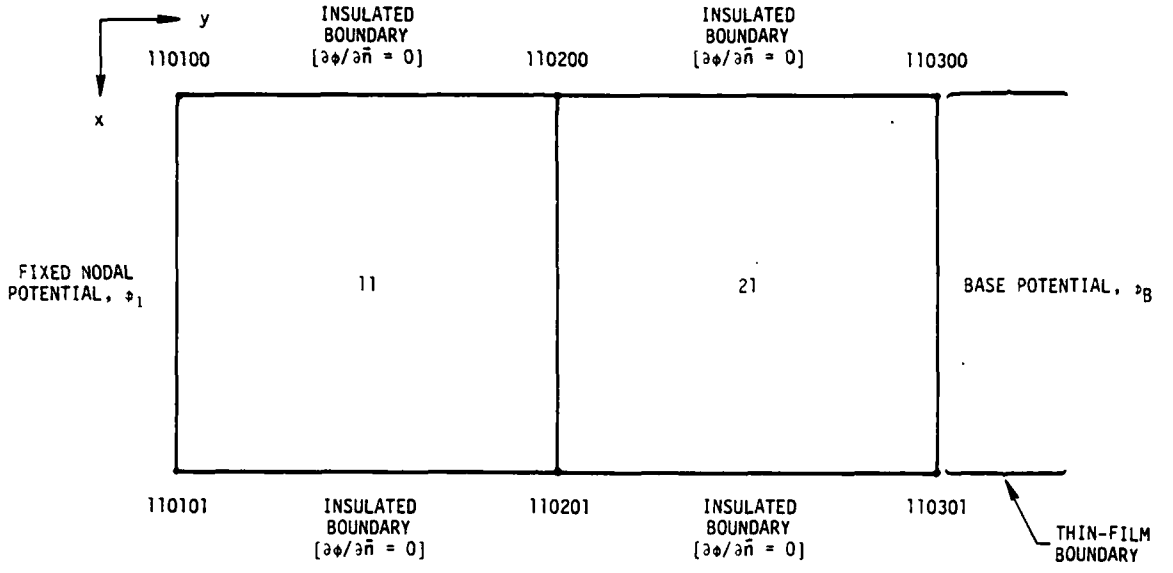

Figure 3. Finite-Element Model (FEM) Used for Boundary-Element Evaluation

multiplied by a length or area associated with the boundary to obtain current, which would be tedious for large, irregular meshes.

It was observed in an earlier computer run that the CQDMEM element readily accepted and accurately predicted the current density from the nonlinear TABLEM1 card. At issue is the correct geometric and impedance characterization of the polarization layer between the metal surface and the electrolyte. This very thin layer appears to control significantly the amount of current density and the potential states (voltage) at which the anodic and cathodic surfaces are operating.

It was, therefore, believed that the boundary element could be modeled by use of a CQDMEM element with extremely small thickness (approximately 10^{-9} units). However, if this very thin quadrilateral element was placed next to one of unit thickness, it would create numerical problems when the conductivity matrix was formulated. Therefore, the model was given a logarithmic thickness distribution (figure 4). This scheme permitted use of the CQDMEM as a boundary element, but it was limited to a thickness of 10^{-6} units due to numerical difficulties. (The units in these examples were in inches.) This element was not considered the best choice because of the many additional elements and grid points needed to model the beaker-pitting situation.

The COSMIC version of NASTRAN possesses a boundary element called CHBDY, explicitly intended for use in modeling boundary effects. It was more attractive than the other elements for this application because it did not require

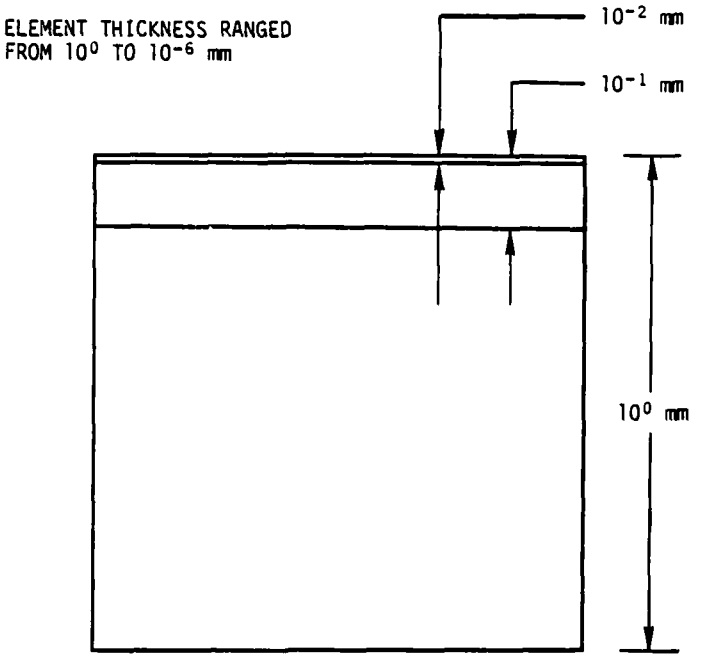

Figure 4. Logarithmic Thickness Distribution

additional nodes nor any correction to heat-flux versus current-density values. The nonlinear polarization trial function assigned to the boundary element is shown in figure 5. The film coefficient was approximated by a combination of step functions, which were chosen because they are representative of anticipated potential-dependent convective values.

The original configuration and computer results are shown in figure 6. It was uncertain from these results whether the program used the average surface potential or the average of the surface and ambient potentials to obtain the voltage-dependent film coefficient.

The voltages of all four boundary nodes were increased on the next run to ensure the program used all potential ranges of the input table. As figure 7 shows, when the calculated average surface potential of 0.5 V confused the program, it used the average value of 5 V rather than choose between 3 or 7 V. This run demonstrated the dangers of discontinuities in nonlinear property tables and showed the program accessing the table with average surface voltage rather than average film potential.

Figure 8 shows the last case, using CQDMEM and CHBDY with increased surface potentials. As expected, the property table yielded a film coefficient of 7, and the element conservation of current (equation (1)) was maintained. It appears that a single-line CHBDY element does not incorporate the nonlinear

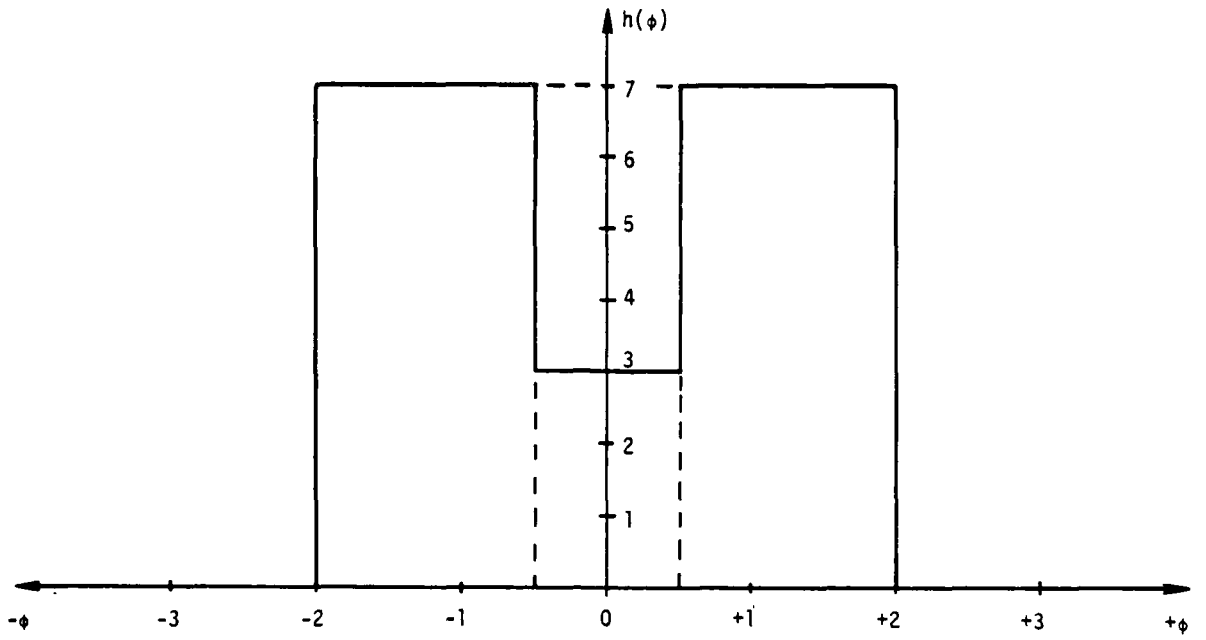

Figure 5. Tabular Function of Nonlinear Convection Coefficient Versus Potential

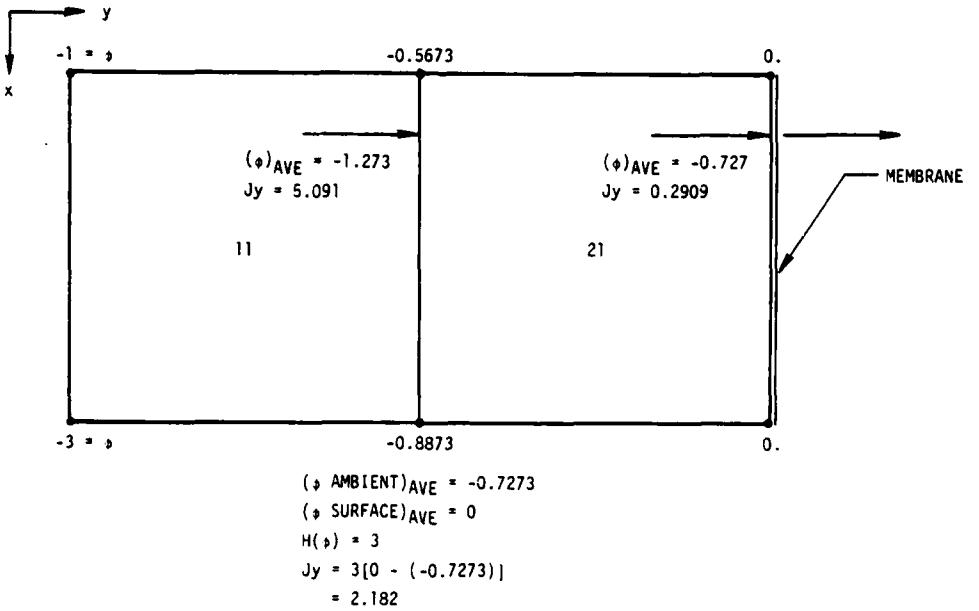

Figure 6. Original Configuration

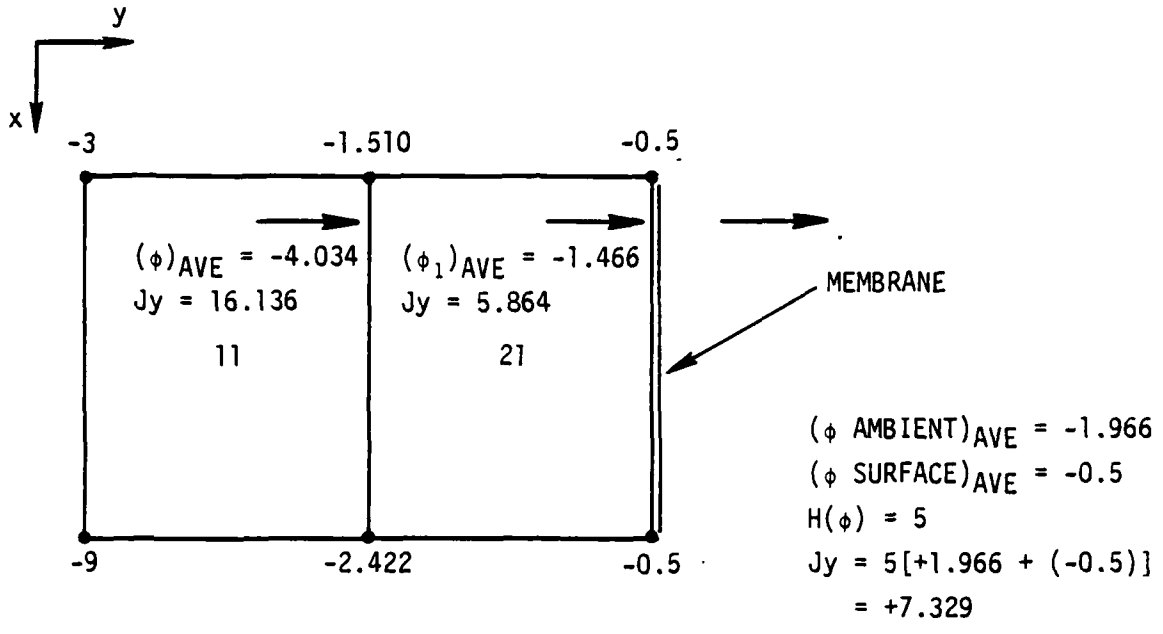

Figure 7. Increased Boundary Potentials

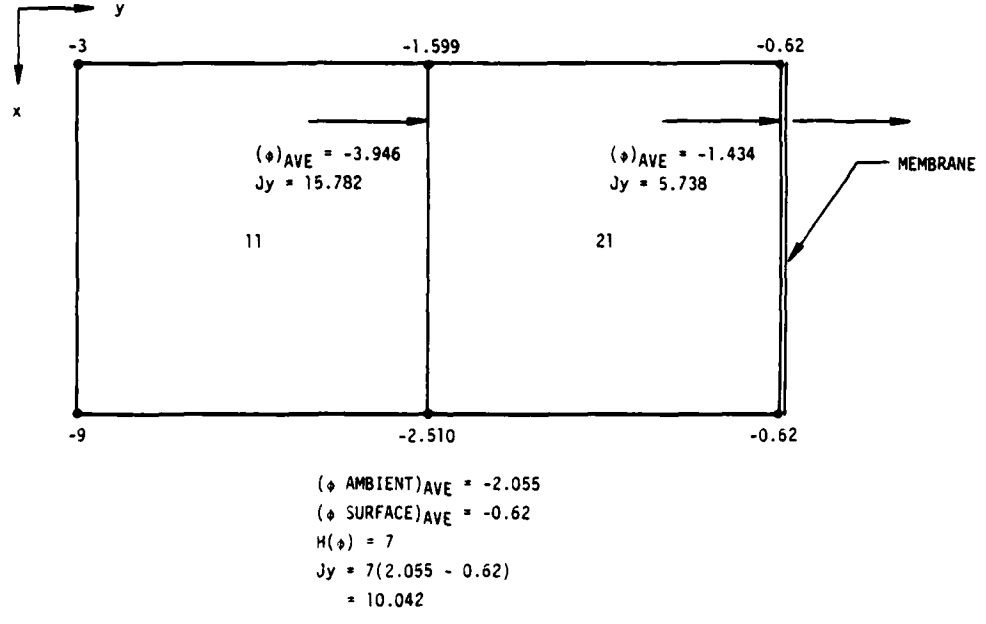

Figure 8. Increased Surface Potential

values from the TABLEM1 in a satisfactory manner. It is possible that the area CHBDY element in an eventual beaker-electrode model that uses an area element could be more successful. This alternative, of course, must be determined analytically.

In each of the FEM's mentioned, the analysis was performed with CQDMEM, CELAS2, and CHBDY elements. It was difficult to determine whether the nonlinear modeling problems were caused by poorly defined boundary conditions, improper reading by COSMIC/NASTRAN of nonlinear tables due to lack of diagnostics, or by numerical problems due to a difference algorithm within COSMIC/NASTRAN (appendix A, pages 8.4-1 to 8.4-12, in the NASTRAN Theoretical Manual, which addresses nonlinear forcing functions and medium matrices).[18] Convergence can be a problem if some of the numerical parameters are not properly chosen. However, a number of guidelines have been suggested that generally provide stability and convergence in the solution set.[18]

A new solution technique was developed that relies on the polarization behavior of the given electrode material. For example, assume that an anodic material behaves as function $f_A(\phi,i)$ in figure 9 and that the cathodic electrode behaves as $f_C(\phi,i)$, where ϕ is the voltage in volts and i is the current density in amperes/meter^2. Both functions are determined empirically. The values ϕ_C and ϕ_A are the constant open-circuit potentials (i = 0 A) for each electrode material. It will be assumed that $f_A(\phi,i)$ and $f_C(\phi,i)$ were generated within the same electrolyte under identical temperatures and conductivities. Therefore, if these two materials are forced to react with each other, the newly coupled system must operate at some equilibrium level designated by line A-A', as indicated in figure 9. Line A-A' corresponds to a constant current, in which the current leaving the anode must arrive at the cathode to satisfy continuity, if all other boundary surfaces are perfectly insulated. Unfortunately, the position of line A-A' is not known a priori. If a secant-slope relationship between the potentials and the currents is employed, the reduction curve for the cathode can be defined and entered in table 2 for copper. The curves shown in figure 9 are general representations for discussion. The actual curves for copper are shown in figure 2,[19] and the conductive parameter, $h(\phi)$, is listed in tables 2 and 3 for the secant-slope and tangent-slope definitions, respectively.

Polarization curves represent a relative voltage potential as a function of current density for immersed electrode materials in electrolyte. Such curves indicate expected oxidation/reduction behavior for a given electrode that is subject to a fixed set of conditions of the electrolyte (temperature, degree of air saturation, composition of electrolyte, etc.). When two electrodes are placed in an electrolyte, mixed potential theory[17] dictates that, for all the partial oxidation and reduction reactions that constitute an electrochemical system, conservation of current, given in equation (1), must be maintained. This implies that point E and point A will shift in figure 9 to accommodate the influence of complex electrochemical surface geometries. The true reaction for the cathodic surface lies somewhere in the neighborhood of point E, figure 9. In the horizontal direction, the analytical solution to the model is physically constrained within the electrolyte to conserve the total current. Hence, the amount of current leaving the anode must equal the

Table 2. Model of Copper Potential Versus Current Curve*

ϕ (V)	i (A/m^2)	$\Delta\phi$	$h(\phi)$ (A/V per m^2)
+0.1	8×10^1	+0.35	$+2.2857 \times 10^2$
0.0	4×10^1	+0.25	$+1.6 \times 10^2$
-0.1	2.5×10^1	+0.15	$+1.6667 \times 10^2$
-0.2	6×10^{-1}	+0.05	$+1.2 \times 10^1$
-0.3	1.1×10^{-1}	-0.05	-2.2×10^0
-0.4	4×10^{-1}	-0.15	-2.6667×10^0
-0.5	1×10^0	-0.25	-4.0×10^0
-0.6	1×10^0	-0.35	-2.8571×10^0
-0.7	1×10^0	-0.45	-2.222×10^0
-0.8	1×10^0	-0.55	-1.8182×10^0
-0.9	1×10^0	-0.65	-1.5385×10^0
-1.0	1×10^0	-0.75	-1.3333×10^0
-1.1	1×10^0	-0.85	-1.1765×10^0
-1.2	2.5×10^0	-0.95	-2.6316×10^0
-1.3	8×10^0	-1.05	-7.619×10^0
-1.4	2.5×10^1	-1.15	-2.1739×10^1
-1.5	7×10^1	-1.25	-5.6×10^{-1}

*Where $i = h(\phi - \phi_{corr})$ and $\phi_{corrosion} \approx -0.25$ V.
By secant-slope model, $1/h(\phi) = \left\{\phi - \phi_{corr}\right\}/i$.

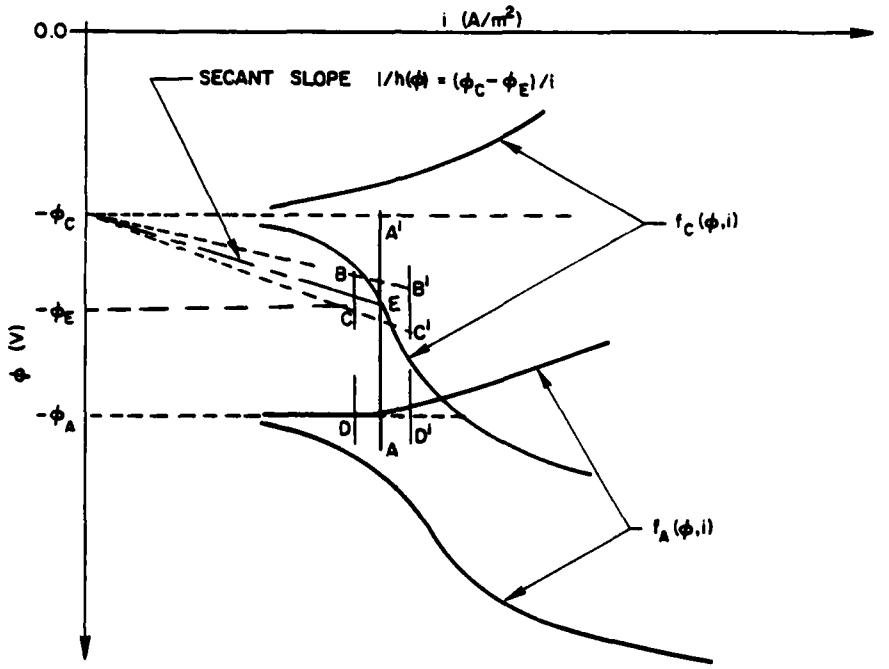

Figure 9. Numerical Determination of Point E

Table 3. Model of Copper ϕ Versus i Curve, Using Tangent Slope

ϕ_1 (V)	ϕ_2 (V)	i_1 (A/m²)	i_2 (A/m²)	$h(\phi) = \left\lvert \frac{i_2 - i_1}{\phi_2 - \phi_1} \right\rvert$
-0.20	-0.25	10^{-3}	7×10^{-2}	1.38
-0.25	-0.30	7×10^{-2}	1.1×10^{-1}	0.80
-0.30	-0.35	1.1×10^{-1}	1.11×10^{-1}	0.02
-0.35	-0.45	1.11×10^{-1}	6.5×10^{-1}	5.39
-0.45	-0.50	6.5×10^{-1}	9×10^{-1}	5.00
-0.50	-1.10	9×10^{-1}	1×10^{0}	0.0952
-1.10	-1.50	1×10^{0}	70	172.5

amount of current arriving at the cathode. This horizontal bound is shown in figure 9 to be lines BCD-B'C'D'.

The variation in the potential state of the cathode about point E is indicated by a lower secant slope, C-C', and an upper secant slope, B-B'. Each secant line is referenced to a differential potential, as indicated by the intersection of line A-A' and lines B-B' and C-C'. The secant slopes B-B' and C-C' intersect at i = 0 on the vertical axis.

By introducing a double-membrane finite-element approach, we place a bound on the cathodic operating potential (point E, figure 9) of a value above (line B-B') and a value below point E. Each membrane possesses the identical nonlinear constitutive information, as measured in figure 2. However, each membrane operates at a different potential value, although both have the same current magnitude. The average potential between the two membranes is defined as the operating potential value for point E (cathodic operating potential). The current flow from the anode to the cathode is governed in this approach by: (1) conservation of current, (2) upper cathodic potential (open-circuit) bound-line ϕ_C = constant (figure 9), (3) lower anodic potential (open-circuit) bound-line ϕ_A = constant (figure 9), and (4) the relevant surface dimensions and geometries causing the shift in points E and A.

EXAMPLE PROBLEM

The physical situation modeled ultimately is a small beaker partially filled with an electrolyte covering two circular continuous electrodes, as shown in figure 10. The area marked A is the anode (iron), C is the cathode (copper), E is the electrolyte, and N is the insulative material. The boundary conditions for the beaker model are shown in figure 11. All the surface areas, represented by $\partial\phi/\partial n = 0$ (no current flow) are nonconductive areas. The electrode surfaces are defined by means of the double membrane explained in the previous section. The analysis is performed by an algorithm within NASTRAN that requires an initial guess for numerical iteration.[18] The mathematical example used to verify the doubled nonlinear membrane approach is shown in figure 12. This checkout model is composed of two AREA4 CHBDY membrane elements spaced 10^{-8} m apart and bounded by two spring-type conductors (electrolyte) on the left and a base cathodic potential on the right. Grid points 13, 4, 14, and 1 represent the open-circuit potential of iron at -0.65 V (anodic). Scalar point 99, on the right, represents the base-metal potential of -0.2 V. The conductive springs are modeled with a value of 4 mho/m, representing sea water. The IR drops in the FEM of figure 12 are calculated in appendix A.

The modeling results are shown in appendix B. The total amount of current from the anode points equals 0.6246616 A. The amount of current passing through the membranes (elements 11 and 12) and arriving at the base metal (scalar point 99) is 0.6246611 A. The continuity of current appears to be satisfied. A similar analysis was completed by replacement of the two spring-type conductors described above with three-dimensional finite elements (figure 13). The same consistency was observed in the results documented in appendix C.

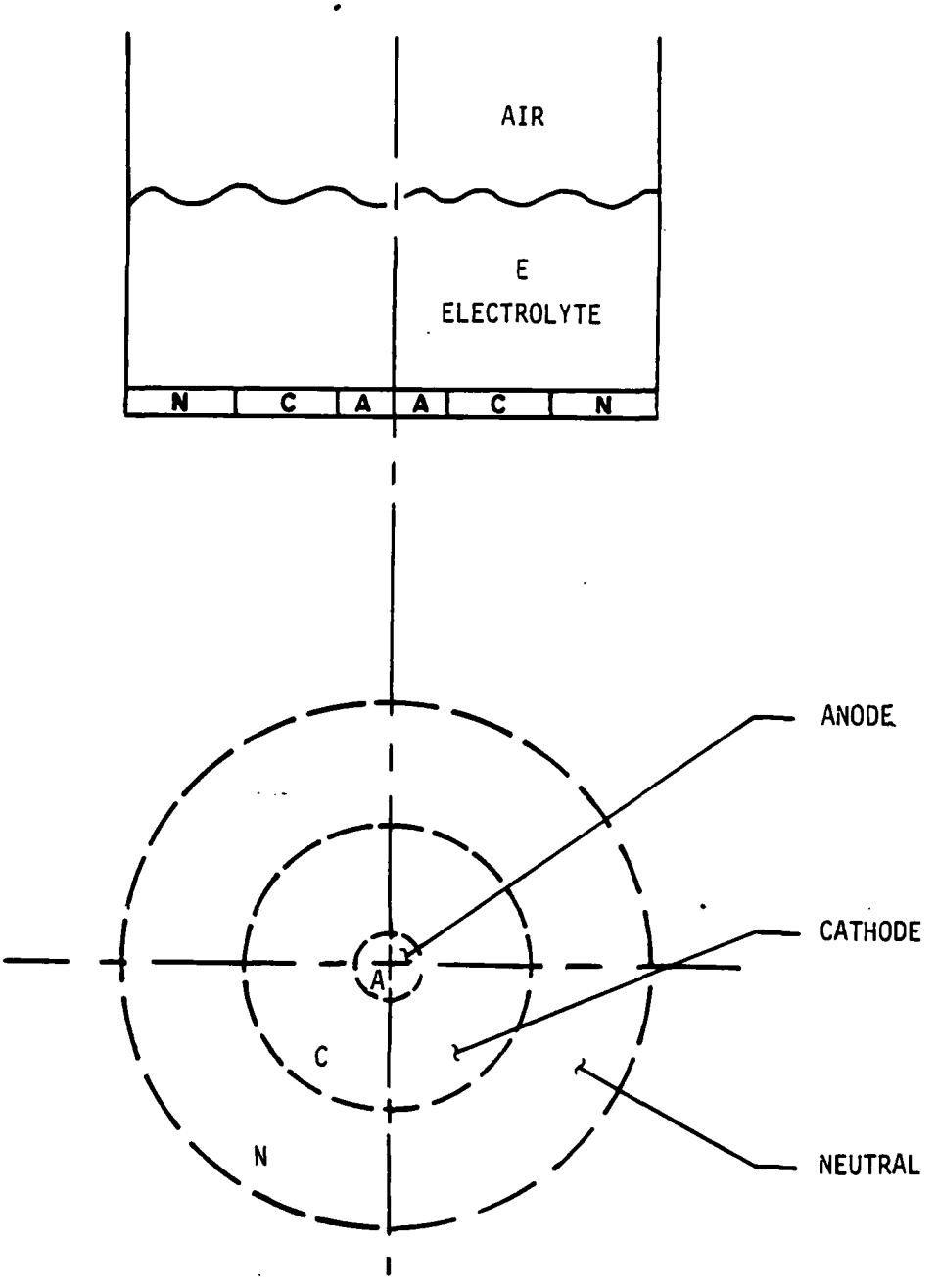

Figure 10. Beaker Model

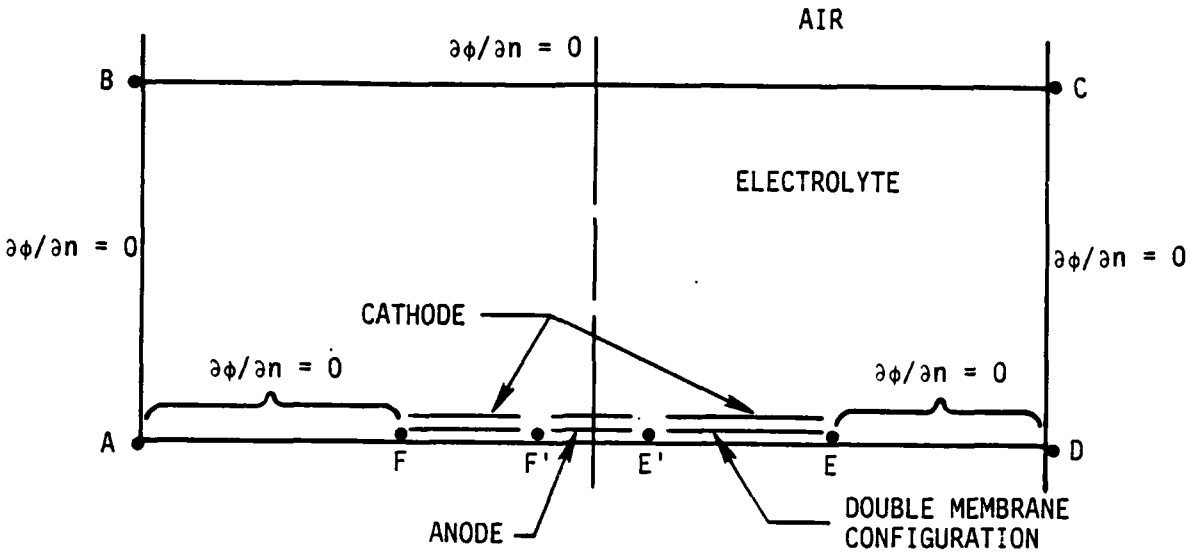

Figure 11. Beaker-Model Boundary Conditions

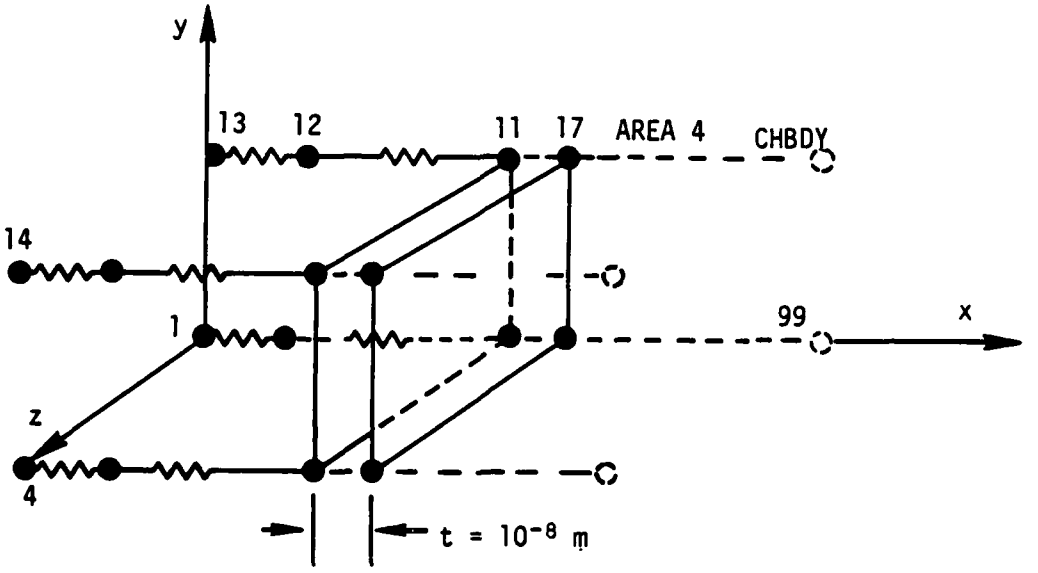

Figure 12. ONR Three-Dimensional CHUB Model,
Current Flow in x Direction

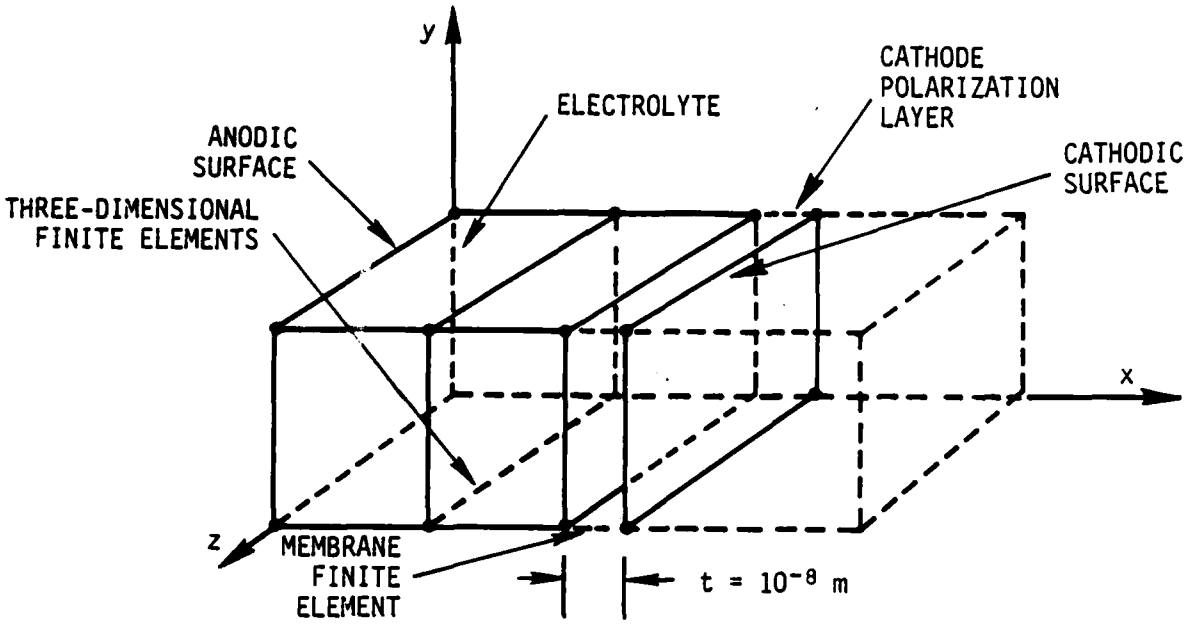

Figure 13. ONR CHEXA Model

This approach should be effective whether it is applied across the anodic or cathodic electrode surfaces. Furthermore, it should not be limited to a specific number of electrodes if they are interacting simultaneously.

RESULTS

The example model used a membrane finite element with a cross section of 1 m^2. The model (figure 12) was assembled in units of meters. From this problem analysis, the resultant current for the defined system was 0.62466 A, which corresponds to a potential in figure 2 of approximately -0.43 V for point E. The potential value of the first and the second membrane are -0.57191 V and -0.28798 V, as shown in appendix B under potential vector. Because these two values represent the lower and upper values of point E (figures 9 and 2), their average indicates the actual potential state of point E. That value is -0.429945 V, from the finite-element analysis; it appears very reasonable, with the nonlinear correspondence shown in figure 2. When the linear conductors in figure 12 are replaced by two three-dimensional solid elements (salt-water electrolyte), as in figure 13, the current is reduced to 0.4108127 A, and the resulting average potential at point E is -0.3512274 V. For a required shift (decrease) in system current requirements, a higher cathodic voltage is observed. This appears consistent with the polarization curve in figure 2.

CONCLUSIONS

It appears that the double membrane approximation for the polarization layer is a satisfactory representation for nonlinear electrode surface behavior. In the mathematical example illustrated in figures 12 and 13, a secant-slope impedance definition was used to calculate current flow near the electrode surfaces. Numerical convergence is realized for equation 5 by means of an integration algorithm[18] strongly analogous to the Newmark B method in structural dynamics. A tangent definition (table 3) of impedance was also used successfully for iron and copper electrodes in conjunction with a double membrane configuration.

A three-dimensional FEM for the beaker will be generated using the double-membrane approach in conjunction with three-dimensional elements for the electrolyte. The beaker model will also contain the effects of nonlinear anodic and cathodic surface behaviors using both secant slope and tangent slope definition for impedance.

REFERENCES

1. N. D. Greene and M. G. Fontana, "A Critical Analysis of Pitting Corrosion," Corrosion, vol. 15, 1959, p. 32t.

2. J. M. Kolotyrkin, "Pitting Corrosion of Metals," Corrosion, vol. 19, no. 8, 1963, pp. 261t-268t.

3. W. D. France, Jr., and N. D. Greene, "Comparison of Chemically and Electrolytically Induced Pitting Corrosion," Corrosion, vol. 26, no. 1, 1970, pp. 1-4.

4. C. Wagner, Die Chemische Reaktion der Metalle Handbuch der Metallphysik J, Vol. 2, Akademische Verlagsgesellschaft Becker und Erler Kom.-Ses., Leipzig, East Germany, 1940, p. 165.

5. K. J. Vetter, Electrochemical Kinetics, Theoretical and Experimental Aspects, Academic Press, New York, NY, 1967, p. 745.

6. B. F. Brown, T. Kruger, and R. W. Staehle (editors), Localized Corrosion, National Association of Corrosion Engineers, Houston, TX, 1974.

7. T. Okada and T. Hashino, "A Contribution to the Kinetic Theory of Pitting Corrosion," Corrosion Science, vol. 17, 1977, p. 671.

8. R. Alkire and D. Siitari, "The Location of Cathodic Reaction During Localized Corrosion," Journal of the Electrochemical Society, vol. 126, 1979, p. 15.

9. E. McCafferty, Mathematical Analysis of Circular Corrosion Cells Having Unequal Polarization Parameters, NRL Report 8107, Naval Research Laboratory, Washington, DC, August 1977.

10. J. W. Fu, "IR-Drop Corrosion in Electrochemical Corrosion Probes Using a Finite-Element Calculation," Paper No. 115, Corrosion/81 - NACE Conference, Toronto, Canada, March 1981.

11. R. S. Munn, Electrochemical Modeling, NUSC Technical Report 6415A, Naval Underwater Systems Center, New London, CT, 28 July 1981.

12. R. G. Kasper and M. G. April, "Electrogalvanic Finite-Element Analysis of Partially Protected Marine Structures," Paper No. 168, Corrosion/82, 22 to 26 March 1982, Houston, TX.

13. J. R. Brauer, "MSC/NASTRAN Analysis of Electric Currents in Cathodic Protection Systems," MSC/NASTRAN User's Conference, Pasadena, CA, 15 to 16 March 1979.

14. R. S. Munn, "A Mathematical Model for a Galvanic Anode Cathodic Protection System," Materials Performance, vol. 21, no. 8, August 1982, pp. 29-36.

15. R. G. Kasper, "Electrochemical Modeling of Three-Dimensional Painted/Unpainted Metal Surfaces Using Finite Element Theory," Corrosion Research Conference, Corrosion/81, 6 April 1981, Toronto, Canada.

16. R. S. Munn, "Modeling of Electrochemical Phenomena for Finite-Element Analysis of Galvanic Systems: I - Use of Applied Current (Conduction) Boundary Condition," NUSC Technical Memorandum No. 831019, Naval Underwater Systems Center, New London, CT (being published).

17. C. Wagner and W. Traud, Zeitschrift für Elektrochemie, vol. 44, 1938, pp. 391.

18. NASTRAN's Theoretical Manual, National Aeronautics and Space Administration, Washington, DC, December 1978, pp. 8.4-1 to 8.4-12.

19. D. C. Bennett, "The Application of Electrode Kinetics to Galvanic Corrosion: I - The Use of Polarization Curves for Predicting Galvanic Corrosion; II - The Galvanogram," MSC Thesis, University of Connecticut, Department of Metallurgy, Storrs, CT, 1973.

Appendix A

CALCULATION OF IR DROPS IN FEM

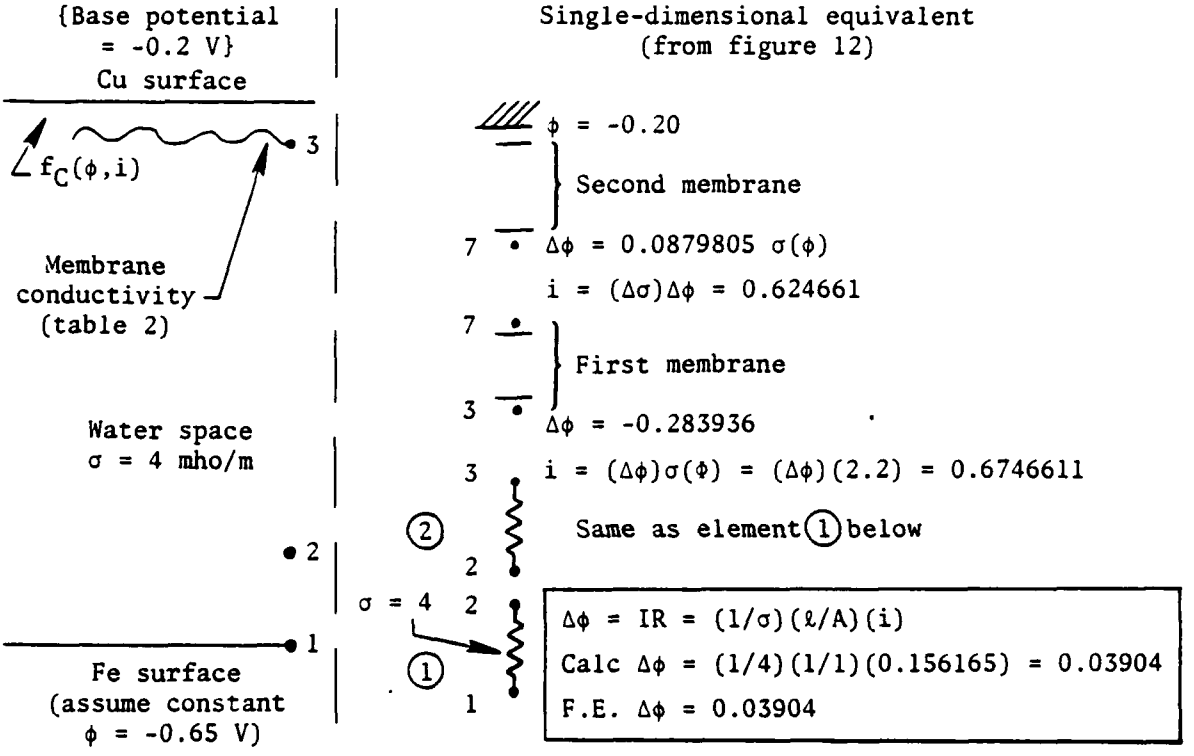

(a) Point E on polarization curve (figure 2) was calculated to be the average of grid points 3 and 7.

$$\phi_E = \frac{-0.571917 - 0.287981}{2} = -0.429949 \text{ V}$$

(b) In equation, $\Delta\phi = (1/\sigma)(\ell/A)(i)$, $\ell = 1$ m, and $A = 1$ m^2.

Appendix B

SAMPLE COMPUTER PRINTOUT FOR ONR CHUB ELEMENTS

This appendix provides a portion of a typical computer printout of ONR CHUB elements for reference.

```
22700        IRON ANODE,COPPER CATHODE IN BEAKER MODEL

22800    0   POTENTIAL VS CURRENT CURVE MODELLED USING SECANT SLOPE METHOD

22900
23000                                    T E M P E R A T U R E   V E C T O R
23100
23200         POINT ID.   TYPE      ID   VALUE     ID+1 VALUE     ID+2 VALUE     ID+3 VALUE     ID+4 VALUE     ID+5 VALUE
23300               1       S     -6.500000E-01  -6.109586E-01  -5.719173E-01  -6.500000E-01  -6.109586E-01  -5.719173E-01
23400               7       S     -2.879805E-01  -2.879805E-01
23500              10       S     -5.719173E-01  -5.719173E-01  -6.109586E-01  -6.500000E-01  -6.500000E-01  -6.109586E-01
23600              16       S     -2.879805E-01  -2.879805E-01
23700              99       S     -2.000000E-01
23800    1   NONLINEAR OHMS LAW                                                  MARCH  17, 1983   RELEASE  APR. 1982    PAGE
                7
23900        IRON ANODE,COPPER CATHODE IN BEAKER MODEL

24000    0   POTENTIAL VS CURRENT CURVE MODELLED USING SECANT SLOPE METHOD

24100
24200                                F O R C E S   O F   S I N G L E - P O I N T   C O N S T R A I N T
1P
24300
24400         POINT ID.   TYPE      ID   VALUE     ID+1 VALUE     ID+2 VALUE     ID+3 VALUE     ID+4 VALUE     ID+5 VALUE
24500               1       S     -1.561654E-01
24600               4       S     -1.561654E-01
24700              13       S     -1.561654E-01  -1.561654E-01
24800              99       S      6.246611E-01
24900    0
25000        THE NEXT LINK IS NS13
25100    0
25200        THE NEXT LINK IS NS14
25300    1   NONLINEAR OHMS LAW                                                  MARCH  17, 1983   RELEASE  APR. 1982    PAGE
                8
25400        IRON ANODE,COPPER CATHODE IN BEAKER MODEL

25500    0   POTENTIAL VS CURRENT CURVE MODELLED USING SECANT SLOPE METHOD

25600
25700                                H E A T   F L O W   I N T O   H B D V   E L E M E N T S   (CHBDV)
25800
1P
25900
26000                          ELEMENT-ID      APPLIED-LOAD       CONVECTION        RADIATION          TOTAL
26100                                11       0.000000E+00      6.246611E-01      0.000000E+00      6.246611E-01
26200                                12       0.000000E+00      6.246612E-01      0.000000E+00      6.246612E-01
26300    1                                  * * * END OF JOB * * *
26400
26500
26600        THE NEXT LINK IS NS01
1
```

Appendix C

SAMPLE COMPUTER PRINTOUT FOR ONR CHEXA ELEMENTS

This appendix provides a portion of a typical computer printout of ONR CHEXA elements for reference.

```
>22800
22800
$P
22900                                        T E M P E R A T U R E   V E C T O R
23000
23100        POINT ID.   TYPE      ID   VALUE     ID+1 VALUE     ID+2 VALUE     ID+3 VALUE     ID+4 VALUE     ID+5 VALUE
23200                1      S     -6.500000E-01  -5.472968E-01  -4.445938E-01  -6.500000E-01  -5.472968E-01  -4.445938E-01
23300                7      S     -2.578609E-01  -2.578609E-01
23400               10      S     -4.445938E-01  -4.445938E-01  -5.472968E-01  -6.500000E-01  -6.500000E-01  -5.472968E-01
23500               16      S     -2.578609E-01  -2.578609E-01
23600               99      S     -2.000000E-01
23700   1    NONLINEAR OHMS LAW                                                    APRIL  26, 1983   RELEASE  APR. 1982    PAGE
     7
23800        IRON ANODE,COPPER CATHODE IN BEAKER MODEL

23900   0    POTENTIAL VS CURRENT CURVE MODELLED USING SECANT SLOPE METHOD

24000
24100                                F O R C E S   O F   S I N G L E - P O I N T   C O N S T R A I N T
24200
24300        POINT ID.   TYPE      ID   VALUE     ID+1 VALUE     ID+2 VALUE     ID+3 VALUE     ID+4 VALUE     ID+5 VALUE
24400                1      S     -1.027034E-01
$P
24500                4      S     -1.027033E-01
24600               13      S     -1.027033E-01  -1.027032E-01
24700               99      S      4.108124E-01
24800   0
24900        THE NEXT LINK IS NS13
25000   0
25100        THE NEXT LINK IS NS14
25200   1    NONLINEAR OHMS LAW                                                    APRIL  26, 1983   RELEASE  APR. 1982    PAGE
     8
25300        IRON ANODE,COPPER CATHODE IN BEAKER MODEL

25400   0    POTENTIAL VS CURRENT CURVE MODELLED USING SECANT SLOPE METHOD

25500
25600                                H E A T   F L O W   I N T O   H B D Y   E L E M E N T S   (CHBDY)
25700
25800
25900                          ELEMENT-ID      APPLIED-LOAD       CONVECTION        RADIATION          TOTAL
26000                                  11      0.000000E+00      4.108123E-01      0.000000E+00      4.108123E-01
$P
26100                                  12      0.000000E+00      4.108123E-01      0.000000E+00      4.108123E-01
26200   1    NONLINEAR OHMS LAW                                                    APRIL  26, 1983   RELEASE  APR. 1982    PAGE
     9
26300        IRON ANODE,COPPER CATHODE IN BEAKER MODEL

26400   0    POTENTIAL VS CURRENT CURVE MODELLED USING SECANT SLOPE METHOD

26500
26600                    F I N I T E   E L E M E N T   T E M P E R A T U R E   G R A D I E N T S   A N D   F L U X E S
26700
26800        ELEMENT-ID   EL-TYPE       X-GRADIENT       Y-GRADIENT       Z-GRADIENT        X-FLUX           Y-FLUX          Z-FLUX
26900                1     HEXA2      1.027032E-01     0.000000E+00     0.000000E+00     -4.108127E-01     0.000000E+00     0.000000
E+00
27000                2     HEXA2      1.027030E-01     0.000000E+00     0.000000E+00     -4.108121E-01     0.000000E+00     0.000000
E+00
27100   1                                        * * * END OF JOB * * *
27200
27300
27400        THE NEXT LINK IS NS01
$
```

INITIAL DISTRIBUTION LIST

Addressee	No. of Copies
Brookhaven National Laboratory (H. S. Isaacs)	1
NAVSEA, 05R25 (H. Vandervelt), 05E1 (W. Strasburg)	2
Lehigh University (H. Leidheiser)	1
DTNSRDC (B. Bieberich, H. P. Hack, W. Andahazy)	3
NRL, 6314 (E. McCafferty)	1
BK Dynamics (J. Fitzgerald)	1
ONR, 431 (P. Clarkin)	1
DTIC	2